J. Phys.: Condens. Matter **19** (2007) 436205 (12pp) doi:10.1088/0953-8984/19/43/436205

Neutron diffraction and ^{119}Sn Mössbauer study of $Sm_3Ag_4Sn_4$

C J Voyer[1], D H Ryan[1], J M Cadogan[2], L M D Cranswick[3], M Napoletano[4], P Riani[5] and F Canepa[6]

[1] Centre for the Physics of Materials and Physics Department, McGill University, Montréal, QC, H3A 2T8, Canada
[2] Department of Physics and Astronomy, University of Manitoba, Winnipeg, MB, R3T 2N2, Canada
[3] Canadian Neutron Beam Centre, National Research Council, Chalk River Laboratories, ON, K0J 1J0, Canada
[4] Dipartimento di Chimica e Chimica Industriale, Via Dodecaneso 31, 16146 Genova, Italy
[5] INSTM and Dipartimento di Chimica e Chimica Industriale, Via Dodecaneso 31, 16146 Genova, Italy
[6] F. Canepa DCCI—Dipartimento di Chimica e Chimica Industriale and CNR—Unità di Genova, Via Dodecaneso 31, 16146 Genova, Italy

Received 3 August 2007
Published 26 September 2007
Online at stacks.iop.org/JPhysCM/19/436205

Abstract

The magnetic properties of $Sm_3Ag_4Sn_4$ have been investigated using bulk magnetization, ^{119}Sn Mössbauer spectroscopy and neutron diffraction. We find that the Néel temperature (T_N) is 26.0(5) K, well above the value of ∼9 K previously determined using magnetic susceptibility measurements. Neutron diffraction data indicate that the Sm moments most likely adopt either the $I_Pmm'm$ or I_Pmmm' magnetic space groups, neither of which allows order at the 2d site, in marked contrast to the vast majority of other compounds in the $R_3T_4X_4$ family. Transferred hyperfine field models suggest that the I_Pmmm' is the only group that is consistent with the ^{119}Sn Mössbauer results. We derive a samarium moment of $0.47 \pm 0.10\ \mu_B$ on the Sm 4e site at 3 K. ^{119}Sn Mössbauer spectroscopy shows that the system undergoes a spin reorientation transition at 8.3(3) K, where the moments rotate towards the a-axis.

(Some figures in this article are in colour only in the electronic version)

1. Introduction

Members of the ternary rare earth compound family $R_3T_4X_4$ (where R is a rare earth, T = Cu, Ag, Au, and X = Si, Ge, Sn) have been extensively studied due to their rich variety of magnetic behaviour [1–5]. They crystallize in the orthorhombic $Gd_3Cu_4Ge_4$-type structure (space group $Immm$, #71) [6], with the rare earth atoms occupying two crystallographically distinct sites (2d and 4e), the transition metal (T) on the 8n site and the X atoms filling the 4f and 4h sites.

 © 2007 IOP Publishing Ltd Printed in the UK

Table 1. Atomic positions for $Sm_3Ag_4Sn_4$ derived from Cu Kα x-ray diffraction data at room temperature. The space group is *Immm*, #71 ($Gd_3Cu_4Ge_4$-type) consistent with other $R_3T_4X_4$ compounds.

Atom	Site	x	y	z
Sm	2d	$\frac{1}{2}$	0	$\frac{1}{2}$
Sm	4e	0.1294(13)	0	0
Ag	8n	0.3279(10)	0.1987(22)	0
Sn	4f	0.2149(14)	$\frac{1}{2}$	0
Sn	4h	0	0.1925(27)	$\frac{1}{2}$

Some members of this diverse compound family exhibit simultaneous order of both rare earth sublattices [3, 4, 7], while others have separate ordering temperatures for each sublattice [7–10]. In many cases there are additional changes in the magnetic structure on further cooling [1, 3, 7, 8, 10] and one example of a coupled first-order magnetostructural transition has also been reported [2, 11]. Where the two R sublattices order separately, the R moments on the 2d sites generally order at a higher temperature than those on the 4e sites [9, 10], and in many cases, no ordering has been detected at the 4e site down to the lowest temperatures explored (typically ∼1.7 K) [8]. This ordering sequence ($^{2d}T_N > {}^{4e}T_N$) is somewhat surprising given that the 2d site would appear to be the more isolated of the two as it is fully coordinated by T and X atoms and has no rare earth nearest neighbours. By contrast, the 4e site has a single 4e rare earth as a first neighbour. So far, only a few systems have been found that have 4e sublattice ordering without magnetic order of the 2d sublattice ($Pr_3Mn_4Sn_4$, $Nd_3Mn_4Sn_4$ [8] and $Nd_3Cu_4Ge_4$ [3]).

A final complication in the $R_3T_4X_4$ family derives from the difficulty in unambiguously determining the ordering temperature from simple bulk magnetic measurements (magnetization and susceptibility). In some cases, the signal from the initial ordering is weak or absent, and a subsequent magnetic reorientation provides a more definitive marker, leading to the misidentification of the ordering temperature [1]. Where neutron diffraction data are available, this error is readily corrected. However, for Gd-based compounds, the high absorption cross-section of natural gadolinium makes neutron-based methods challenging and they are rarely attempted. A recent example is provided by $Gd_3Ag_4Sn_4$, where initial studies pointed to an ordering temperature of 8 K [12], but subsequent ^{119}Sn Mössbauer work showed this event to be a reorientation transition, with the actual onset of magnetic order occurring at ∼29 K [1].

Here we show, using ^{119}Sn Mössbauer spectroscopy and neutron diffraction, that the reported ordering temperature of ∼9 K [12] for $Sm_3Ag_4Sn_4$ actually marks a spin reorientation transition and that the onset of magnetic order occurs at 26.0(5) K.

2. Experimental methods

Stoichiometric amounts of Sm rods, 99.9 mass% purity, Ag ingots and Sn bars, respectively, 99.999 mass% purity, were placed in a tantalum crucible which was sealed by arc welding under purified argon. They were then melted in an induction furnace, quenched in water and annealed at 873 K for 20 days. Electron microprobe analysis and Cu Kα x-ray diffraction confirmed that the majority phase was the orthorhombic $Gd_3Cu_4Ge_4$-type phase with less than 6% of the ζ-phase $Ag_{79}Sn_{21}$ present. The x-ray patterns were fitted with GSAS [13] via the EXPGUI [14] user interface, and yielded lattice parameters of $a = 15.300(3)$ Å, $b = 7.324(2)$ Å and $c = 4.597(1)$ Å, consistent with other $R_3Ag_4Sn_4$ compounds [1–5, 12]. The site coordinates are listed in table 1, and the fit is shown in figure 1.

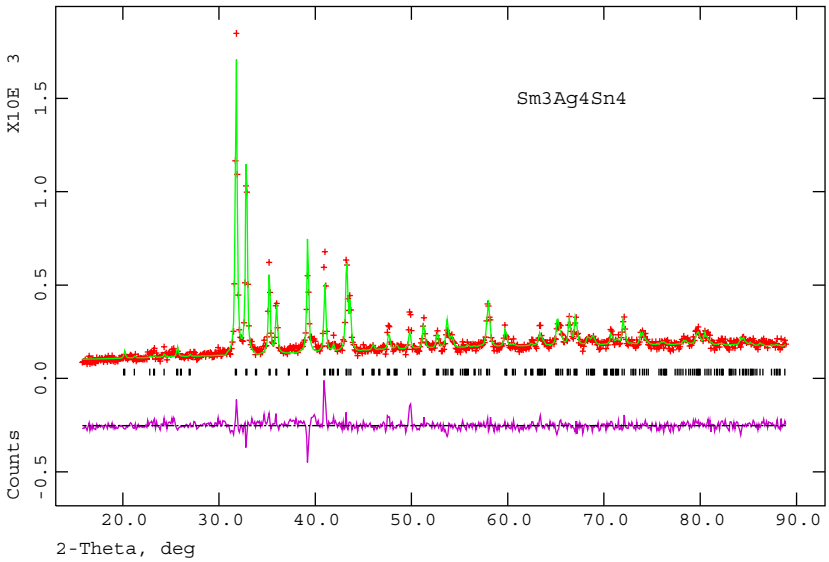

Figure 1. The Cu Kα x-ray diffraction pattern obtained at room temperature. The difference between the experimental data and the calculated pattern is also shown, as well as Bragg markers indicating allowed reflections.

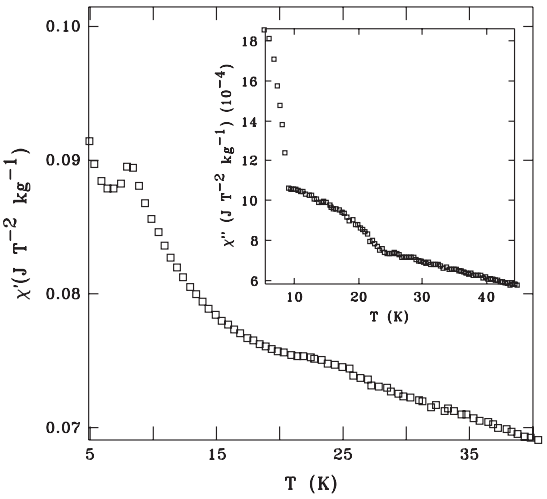

Figure 2. Temperature dependence of the in-phase ac susceptibility (χ') in $Sm_3Ag_4Sn_4$, acquired with a field of 1 mT at 337 Hz. The inset shows the out-of-phase signal χ'', acquired at 977 Hz on a much larger (0.5 g) sample. The reorientation transition at 8.25(15) K is evident in both channels, while only χ'' shows a clear signature of the bulk ordering at 24(1) K.

Initial magnetic characterization by ac susceptibility (χ'), shown in figure 2, reveals a clear peak at 8.25(15) K, close to the 9 K value previously attributed to the onset of antiferromagnetic (AF) order in this compound [12]. An extremely weak departure from Curie–Weiss $1/T$ behaviour may be present between 20 and 25 K, and this is confirmed by the out-of-phase signal (χ'') shown in the inset to figure 2, where a marked increase is apparent at 24(1) K.

As we show below, the onset of magnetic order occurs at ∼26 K, while the 8.25(15) K event marks a spin reorientation.

^{119}Sn Mössbauer spectra were collected in transmission mode on a constant acceleration spectrometer using a 0.4 GBq ^{119m}Sn $CaSnO_3$ source with the sample in a helium flow cryostat. A 25 μm Pd filter was used to absorb the Sn Kα x-rays also emitted by the source. The spectrometer was calibrated using a ^{57}Co Rh source and an α-Fe foil. Typical linewidths were 0.6 mm s^{-1} full width at half maximum (FWHM), consistent with a $CaSnO_3$ standard.

The spectra were fitted using a conventional nonlinear least-squares minimization routine. Since we were fitting spectra through the magnetic transition where the hyperfine magnetic field and quadrupole shift (Δ) have comparable sizes, a perturbative approach was not appropriate, and so line positions and intensities were calculated from an exact solution to the full Hamiltonian with combined magnetic dipole and electric quadrupole interactions [15].

Neutron diffraction measurements were made using the C2 multi-wire powder diffractometer at Chalk River Laboratories, Ontario, at a wavelength of 2.3719 Å. The very large absorption cross-section in Sm ($\sigma_{abs} = 5922(56)$ barn) leads to a $1/e$ absorption thickness of ∼140 μm for $Sm_3Ag_4Sn_4$, and so precludes mounting in a conventional 5 mm diameter cylindrical sample holder. We therefore used a large-area flat-plate holder with single-crystal silicon windows that was developed to work with highly absorbing samples [16]. This holder allowed us to place about 1.6 g of sample in the 8 cm × 2.4 cm beam and obtain a usable scattering signal. Cooling was achieved using a closed-cycle refrigerator.

3. Results and discussion

3.1. ^{119}Sn Mössbauer spectroscopy

As both tin sites in the $Gd_3Cu_4Ge_4$-type structure adopted by $Sm_3Ag_4Sn_4$ have first neighbours from each of the two samarium sublattices, the transferred hyperfine field, $\mathbf{B}_{hf}$, observed at each tin site by ^{119}Sn Mössbauer spectroscopy is sensitive to magnetic ordering on both samarium sites in the compound.

Examination of the 2.2 K spectrum, shown in figure 3, reveals two magnetically split, equal-area components, consistent with the populations of the two crystallographic sites for Sn (4f and 4h). Each component has a distinct hyperfine field (8.44(2) and 3.11(2) T), comparable to those seen in $Gd_3Ag_4Sn_4$ [1], with no significant non-magnetic contribution present. We conclude that all of the tin in the sample is in the primary $Sm_3Ag_4Sn_4$-phase and that each of the two crystallographically distinct tin sites also occupies a magnetically unique site (there is no apparent line broadening or subsplitting of the components that might reflect a more complex magnetic environment).

The spectrum was fitted by fixing the magnitude of the quadrupole shift, $|\Delta|$, to 0.87 mm s^{-1} for both subspectra. This value was obtained from spectra taken in the paramagnetic state (at 35 K) where only a simple doublet is observed, indicating that the electrostatic environments of the two tin sites are quite similar and could not be resolved. Since a paramagnetic ^{119}Sn Mössbauer spectrum can only reveal the *magnitude* of Δ, the negative sign of Δ for both subspectra was established by fitting the spectra in the magnetically ordered state at 2.2 K. Due to the point groups of the Sn 4f and Sn 4h sites (2*mm* and *m*2*m* respectively), we expect the principal axis of the electric field gradient tensor, V_{zz}, to be parallel to one of the crystallographic axes. Point-charge calculations suggest that V_{zz} points along the *b*-axis for the Sn 4f site and along the *c*-axis for the Sn 4h site. The electric field gradient asymmetry parameter, η, was found to be small (<0.2) in both cases. η was therefore set to zero and not

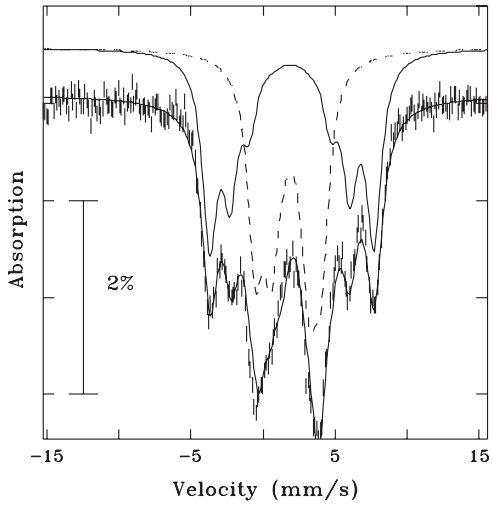

Figure 3. ^{119}Sn Mössbauer spectrum of $Sm_3Ag_4Sn_4$ acquired at 2.2 K. The solid line through the data is a full Hamiltonian fit described in the text. The two equal-area components making up the fit are shown displaced above the data. The solid line represents the high-field component while the dashed line shows the form of the low-field component.

refined in the initial analysis of the Mössbauer spectra. This choice permits us to determine the angle, ϑ, between V_{zz} and $\mathbf{B}_{\rm hf}$, but not the polar angle, ϕ.

The left panel of figure 4 shows the progression of the ^{119}Sn Mössbauer spectra with temperature. We can clearly see that the magnetic splitting persists well above the ∼9 K transition temperature inferred from susceptibility data. No significant (<2%) impurity was detected at any temperature, indicating that the magnetic behaviour observed here reflects bulk ordering in the primary phase. Moreover, the spectral areas remain equal throughout, evidence that we are observing the evolution of $\mathbf{B}_{\rm hf}$ at each Sn site (4h and 4f) distinctly. From our fits, we obtain the temperature dependence of $\mathbf{B}_{\rm hf}$ for each site and the corresponding angle ϑ between $\mathbf{B}_{\rm hf}$ and V_{zz}, shown on the right panels of figure 4.

The temperature dependence of $\mathbf{B}_{\rm hf}$ for each component was fitted to a sum of two $J = \frac{5}{2}$ (the value for Sm^{3+}) Brillouin functions. This yields Néel temperatures ($T_{\rm N}$) of 26.2(4) and 25.2(1.3) K from the high-field and low-field sites, respectively, giving a weighted average transition temperature of $T_{\rm N} = 26.0(5)$ K. Similarly, the low-temperature event occurs at 8.6(3) and 8.0(3) K for an average of 8.3(3) K, and corresponds precisely with the 8.25(15) K peak seen in $\chi'(T)$ (figure 2). This event marks an abrupt change in the direction of $\mathbf{B}_{\rm hf}$ at both Sn sites, and must in turn reflect a change in the surrounding Sm moment directions. Such behaviour has been observed in other compounds such as $Gd_3Ag_4Sn_4$ [1], $Tb_3Ag_4Sn_4$ [2] and $Dy_3Ag_4Sn_4$ [4], and given the presence of magnetic order well above 8 K, the ^{119}Sn Mössbauer data clearly show that the sharp feature seen in figure 2 is not actually due to the onset of long-range magnetic order, but rather marks a magnetic reorientation transition.

We observe no change in linewidth on passing through the 8 K event, nor are there any changes to the spectral shape that cannot be accounted for by the static Hamiltonian used to calculate the line positions and intensities; we therefore conclude that the magnetic order that we observe in the Mössbauer spectra for 8 K $< T <$ 26 K is static in nature and reflects long-range ordering of the samarium moments. However, as a local probe of magnetic order, Mössbauer spectroscopy cannot definitively show that long-ranged magnetic order is present. For this information, we turn to neutron diffraction.

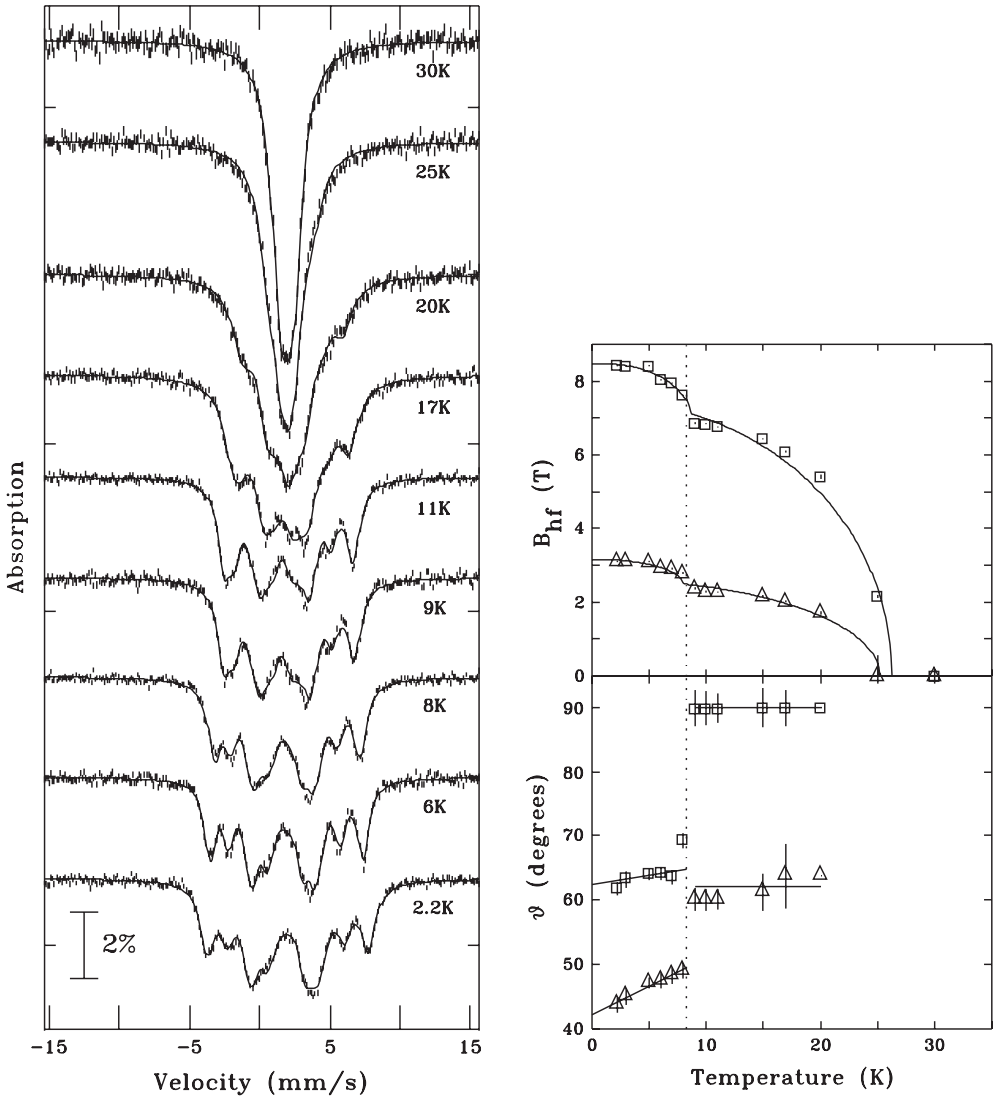

Figure 4. Left: ^{119}Sn Mössbauer spectra of $Sm_3Ag_4Sn_4$. We can clearly see the onset of magnetic order well above 9 K. Right (top): temperature dependence of the hyperfine field $\mathbf{B}_{hf}$ fitted with a sum of two $J = \frac{5}{2}$ Brillouin functions; (bottom): the angle (ϑ) between V_{zz} and $\mathbf{B}_{hf}$. Solid lines are guides to the eye.

3.2. Neutron scattering

The small sample combined with the large absorption cross-section of natural samarium leads to relatively weak scattering from the sample. The situation is exacerbated by both the very small coherent scattering length for Sm (0.00(5) fm), which will lead to reduced structural scattering, and the small magnetic moment (∼0.5 μ_B) expected on the Sm atoms in metallic compounds [17–19], which will yield very weak magnetic scattering.

Figure 5 shows the neutron diffraction pattern of $Sm_3Ag_4Sn_4$ taken in the paramagnetic state (50 K) at a wavelength of 2.3719 Å. As anticipated, the signal is quite weak, with the

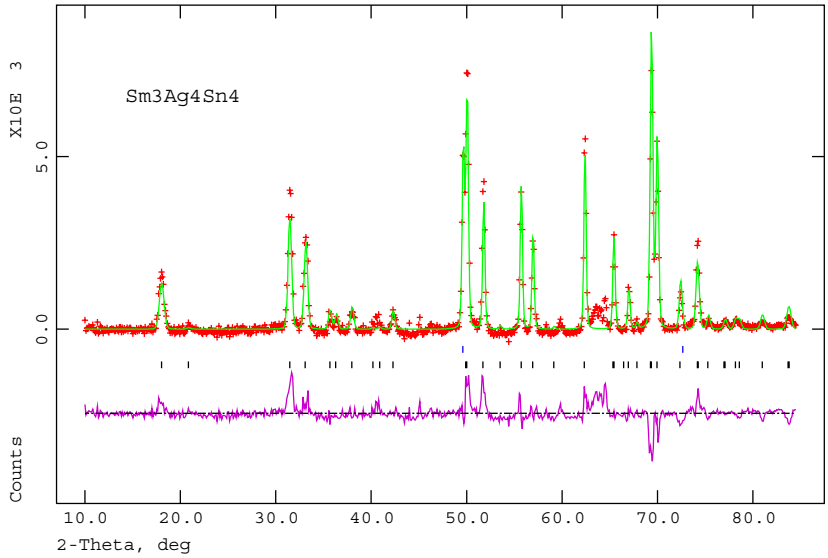

Figure 5. Neutron diffraction pattern taken at 50 K (paramagnetic state). A Rietveld refinement is shown as a solid line through the data with the difference between the calculated and observed pattern shown below. Bragg markers for the primary $Sm_3Ag_4Sn_4$ phase (bottom) and the sample holder (top) are also shown.

strongest structural peaks having a count rate of ∼100 cts h^{-1}. Rietveld refinement of the pattern using GSAS/EXPGUI [13, 14] included a correction to the peak intensities to account for the angle-dependent absorption caused by the flat-plate geometry. Analysis confirmed the structure and lattice parameters established by the x-ray diffraction measurements.

Examination of the 3 K diffraction pattern, shown at the top of figure 6, shows no striking change from the paramagnetic state, although a weak peak near $2\vartheta = 9°$ is visible. The magnetic scattering can be isolated by taking the difference between the patterns at 3 and 50 K (middle curve in figure 6), and we see that the *only* significant magnetic signal is associated with the 9° peak, which can be identified as being due to the (100) reflection. The width of this peak is consistent with both the instrumental resolution function and the structural peaks at higher angles, leading us to conclude that long-ranged magnetic order is definitely established at 3 K in this compound. Furthermore, the presence of this (100) peak indicates that the Sm moments have at least some component in the *bc*-plane.

To determine the magnetic structure of $Sm_3Ag_4Sn_4$ at 3 K, we now consider the 16 magnetic space groups associated with the $Immm$ (#71) crystallographic space group. There are 8 'I' groups, in which moments related by the body-centring translation are parallel, and 8 'anti-I' groups, denoted I_P, in which such moments are anti-parallel. The magnetic ordering modes at the Sm 2d and 4e sites allowed by these 16 magnetic space groups are summarized in table 2, using standard notation.

We recall here that nuclear scattering in an $Immm$ structure does not contribute to peaks for which ($h + k + l$ = odd) so the observation of a purely magnetic (100) peak below 9 K immediately imposes the following constraints on the magnetic ordering in $Sm_3Ag_4Sn_4$:

- at least one of the two Sm sites must order magnetically,
- the magnetic order below 9 K cannot be ferromagnetic,
- the magnetic order below 9 K cannot be directed along the crystal a-axis.

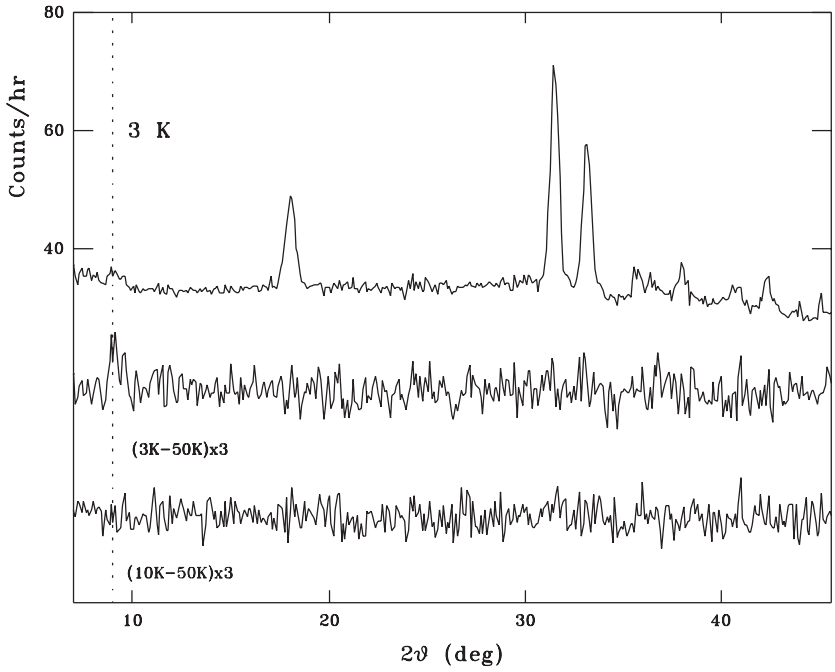

Figure 6. Top: neutron diffraction pattern for $Sm_3Ag_4Sn_4$ taken at 3 K showing a weak magnetic peak at $2\vartheta = 9^\circ$ (dotted line). Middle: difference between the 3 and 50 K patterns (scaled by a factor of 3) to emphasize the magnetic peak. Bottom: difference between the 10 and 50 K patterns enlarged by the same factor of 3, showing no apparent magnetic signal. All measurements were made at a wavelength of 2.3719 Å.

Table 2. Magnetic space groups derived from the *Immm* crystal space group. The 2d atomic positions are $(\frac{1}{2}\ 0\ \frac{1}{2})$ and $(0\ \frac{1}{2}\ 0)$. The 4e positions are $(x\ 0\ 0)$, $(-x\ 0\ 0)$, $(x+\frac{1}{2}\ \frac{1}{2}\ \frac{1}{2})$ and $(-x+\frac{1}{2}\ \frac{1}{2}\ \frac{1}{2})$.

n	Magnetic space group	2d order	2d sequence	4e order	4e sequence
1	$Immm$	0		0	
2	$Immm'$	0		b	$+-+-$
3	$Imm'm$	0		c	$+-+-$
4	$Im'mm$	0		0	
5	$Imm'm'$	a	$++$	a	$++++$
6	$Im'mm'$	b	$++$	b	$++++$
7	$Im'm'm$	c	$++$	c	$++++$
8	$Im'm'm'$	0		a	$+-+-$
9	I_Pmmm	0		0	
10	I_Pmmm'	0		b	$+--+$
11	$I_Pmm'm$	0		c	$+--+$
12	$I_Pm'mm$	0		0	
13	$I_Pmm'm'$	a	$+-$	a	$++--$
14	$I_Pm'mm'$	b	$+-$	b	$++--$
15	$I_Pm'm'm$	c	$+-$	c	$++--$
16	$I_Pm'm'm'$	0		a	$+--+$

Thus, we may rule out groups 1, 4, 9 and 12 as they do not allow any magnetic order at the Sm sites. We may also rule out groups 5, 8, 13 and 16 as they only allow the 4e

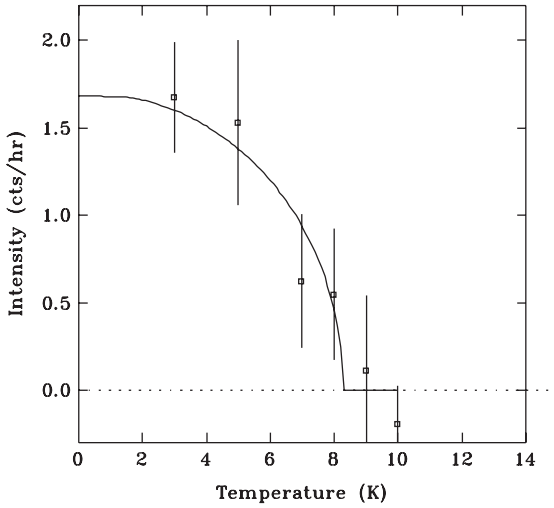

Figure 7. Temperature dependence of the intensity of the (100) reflection at $2\vartheta = 9°$. The solid line is a Brillouin function fit and the transition temperature derived from the fit, 8.3(4) K, is in excellent agreement with the moment reorientation temperature obtained from ^{119}Sn Mössbauer spectroscopy.

site to order along the crystal a-axis, incompatible with the observation of a magnetic (100) peak. As noted above, (100) scattering cannot result from ferromagnetic order, and previous magnetization measurements [12] have shown that $Sm_3Ag_4Sn_4$ exhibits antiferromagnetic order. Thus, we can also rule out the ferromagnetic groups 6 and 7. Of the six remaining candidate magnetic groups (2, 3, 10, 11, 14 and 15) only two (group 10, I_Pmmm', and group 11, $I_Pmm'm$) yield enough intensity on the (100) peak to be consistent with the data shown in figure 6. Remarkably, neither of these groups permits magnetic ordering at the 2d site, setting $Sm_3Ag_4Sn_4$ apart from the vast majority of compounds in the $R_3T_4X_4$ family ($Tb_3Cu_4Ge_4$, $Ho_3Cu_4Sn_4$, $Er_3Cu_4Ge_4$, $Er_3Cu_4Sn_4$ [8], $Er_3Cu_4Si_4$, $Er_3Cu_4Sn_4$ [9], $Tb_3Cu_4Si_4$ [10], $Tb_3Cu_4Sn_4$, $Dy_3Cu_4Ge_4$, $Dy_3Cu_4Sn_4$, $Ho_3Cu_4Ge_4$ [8]) where ordering on the 2d site is either the only form seen, or at least the preferred ordering, with the 4e sites ordering only at a much reduced temperature.

Tracking of the intensity of the 9° peak with temperature (figure 7) shows that it disappears at 8.3(4) K, in perfect agreement with the reorientation temperature measured by ^{119}Sn Mössbauer spectroscopy. It is clear from the bottom curve in figure 6 that no significant magnetic signal is observed at 10 K, despite clear evidence in the Mössbauer spectra that the compound remains ordered until 26 K. Simulation of the nine possible magnetic groups that support AF ordering of the samarium moments reveals that only the two candidate groups for the low-temperature structure (I_Pmmm' and $I_Pmm'm$) yield a strong magnetic signature; the others all lead to multiple weak magnetic peaks. As a result, our failure to detect magnetic scattering above 9 K does not necessarily demand a loss of magnetic order at 8.3(4) K, but rather, when taken with the clear magnetic signal in the ^{119}Sn Mössbauer spectra, it implies a change in magnetic order, with the Sm moments rotating closer to the a-axis. The overall weakness of the magnetic scattering, and the absence of magnetic peaks at 10 K, preclude further analysis of the neutron diffraction data, and we are unable to determine the magnetic structure between 8.3 and 26.0 K.

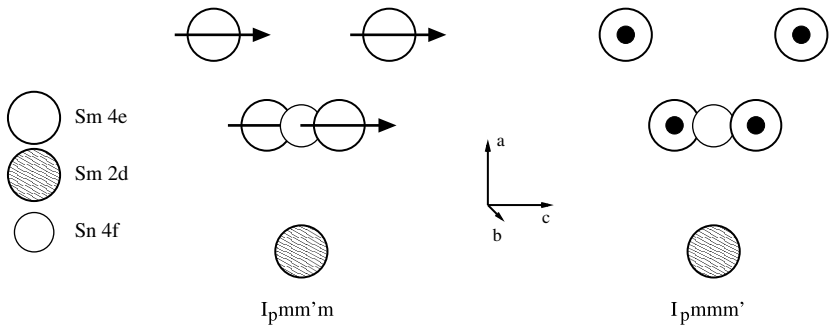

Figure 8. Magnetic environment of the Sn 4f site if the adopted magnetic group is $I_Pmm'm$ (left) or I_Pmmm' (right). The atom symbols are identified at the left. The two Sm 4e atoms above the Sn 4f, and the Sm 2d below it, share a common plane. Additional Sm 4e atoms lie in front of and behind the central Sn 4f. For $I_Pmm'm$, the moments on the 4e site point along $+c$, whereas for I_Pmmm', they point along $+b$ (out of the page).

Table 3. The nearest-neighbour rare earths with their fractional coordinates.

Sn site	Neighbour atom	Interatomic distance (Å)	x	y	z
	Sm 2d	3.289(21)	0	$\frac{1}{2}$	0
4f	Sm 4e	3.310(22)	0.370 59	$\frac{1}{2}$	$-\frac{1}{2}$
	Sm 4e	3.310(22)	0.370 59	$\frac{1}{2}$	$\frac{1}{2}$
	Sm 4e	3.889(23)	0.129 41	1	0
	Sm 4e	3.889(23)	0.129 41	0	0
	Sm 2d	3.218(14)	0	$\frac{1}{2}$	0
	Sm 2d	3.218(14)	0	$\frac{1}{2}$	1
4h	Sm 4e	3.346(16)	0.129 41	0	0
	Sm 4e	3.346(16)	0.129 41	0	1
	Sm 4e	3.346(16)	−0.129 41	0	0
	Sm 4e	3.346(16)	−0.129 41	0	1

3.3. Combining the neutron scattering and ^{119}Sn Mössbauer data

^{119}Sn Mössbauer spectroscopy and neutron diffraction provide distinct yet complementary information on the magnetic ordering in $Sm_3Ag_4Sn_4$ which can be used to refine the choice of magnetic space groups (I_Pmmm' or $I_Pmm'm$). The nearest Sm neighbours to each Sn site are listed in table 3, and the magnetic environments for the two possible magnetic space groups allowed by the neutron diffraction data are depicted in figure 8 for the Sn 4f site, and figure 9 for the Sn 4h site.

If we consider only the isotropic contribution to the transferred hyperfine field we find that neither magnetic group yields a transferred field at the Sn 4h site as the four Sm 4e first neighbours for this site are equidistant and consist of two 'up's and two 'down's, so their effect cancels (figure 9). We must therefore include anisotropic contributions. First expressed in the case of $MnSn_2$ [20], the transferred hyperfine field at the ^{119}Sn nucleus due to neighbouring Mn moments includes both isotropic (simple vector sum over the moments) and anisotropic (dipolar field due to a covalent contribution to the Mn–Sn bonding) terms. A recent study has shown that there is also an anisotropic contribution to the transferred hyperfine field from neighbouring

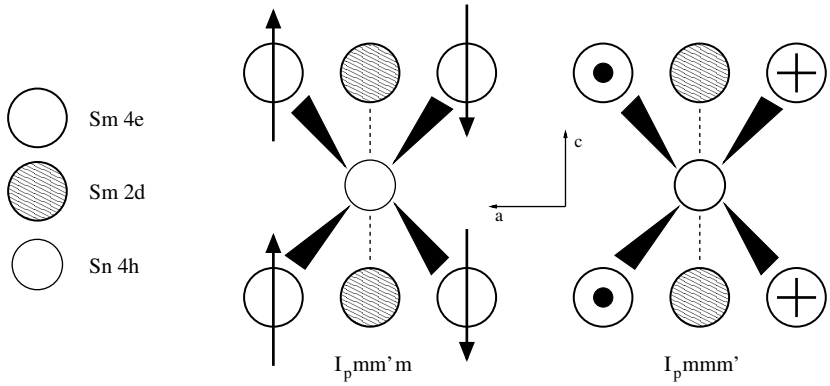

Figure 9. Magnetic environment of the Sn 4h site if the adopted magnetic group is $I_Pmm'm$ (left) or I_Pmmm' (right). The atom symbols are identified at the left. In this sketch there are three distinct depths. The four coplanar 4e atoms are 2.25 Å in front of the Sn 4h site while the two Sm 2d sites are 1.41 Å behind it. For both magnetic groups, the isotropic contribution will be zero; however, the anisotropic contribution cancels only for $I_Pmm'm$.

rare earth moments, and that this field is similar in magnitude to the Mn contribution [21]. The anisotropic term is proportional to the projection of the moment direction onto the position vector between the Sn and Sm atoms. The field is thus maximized if the moment points along the position vector, and zero if it is perpendicular to it.

From figure 8, we can see that for both magnetic groups the isotropic contribution to the transferred hyperfine field at the Sn 4f site will be non-zero, pointing in the $+c$ direction for $I_Pmm'm$ since both Sm 4e moments point in that direction and likewise in the $+b$ direction for I_Pmmm'. The anisotropic contribution is also non-zero for both magnetic groups. The situation at the Sn 4h site (figure 9) is, however, quite different. As noted above, the isotropic contribution cancels for both possible groups. In addition, the anisotropic contribution is zero for the $I_Pmm'm$ structure, with the result that *only* the I_Pmmm' group yields a non-zero transferred hyperfine field at the Sn 4h site, and then only when the anisotropic contribution is taken into account. Rietveld refinement of the 3 K pattern, assuming that the I_Pmmm' structure is correct, yields a samarium moment of $0.47 \pm 0.10\ \mu_B$ on the Sm 4e site[7].

Assuming that the magnetic order below 8 K in $Sm_3Ag_4Sn_4$ follows the I_Pmmm' group, then we should observe a transferred hyperfine field at both Sn sites: 4f along b and 4h along a. If we further assume that our point-charge calculations are correct, then they place V_{zz} along the b-axis for the Sn 4f site and along the c-axis for the 4h site. This analysis predicts that the angle between $\mathbf{B}_{hf}$ and V_{zz} should be $\vartheta = 90°$ at both tin sites; however, this is not consistent with the results shown in the right panel of figure 4. Force-fitting $\vartheta = 90°$ at both sites yields extremely poor fits, and a grid search in both η and the polar angle ϕ did not lead to a better fit to the spectra than is shown in figure 4. While one might appeal to the limited validity of point-charge calculations, the point symmetry of both Sn sites alone leads to $\vartheta = 90°$ or 0° for both magnetic structures that are consistent with the neutron diffraction data. It is therefore likely that some subtlety of the transfer process is being missed. As neutron diffraction is unlikely to yield further information (samples prepared with a less absorbing Sm isotope would be smaller than the one employed here and so would not yield a better signal) the best way forward would

[7] As the $I_Pmm'm$ and I_Pmmm' magnetic structures differ simply by having the Sm 4e moments directed along the c-axis or b-axis respectively, both structures yield the same intensity for the (100) reflection, and the derived Sm moment of $0.47 \pm 0.10\ \mu_B$ is independent of this final choice.

appear to be to use single-crystal samples for ^{119}Sn Mössbauer spectroscopy where the actual moment directions could be established directly.

4. Conclusions

^{119}Sn Mössbauer spectroscopy reveals that the previously determined value for T_N (∼9 K) in $Sm_3Ag_4Sn_4$ was greatly underestimated and that susceptibility provides only a weak signature of the actual bulk ordering at 26.0(5) K. Analysis of the Mössbauer data reveals that the event at 8.3(3) K is in fact a spin reorientation transition.

The neutron diffraction data indicate that the Sm moments, below 8.3 K, adopt a magnetic structure that requires a component in the bc-plane, and is most likely either $I_Pmm'm$ or I_Pmmm'. Neither group allows order at the 2d site, in contrast to the vast majority of other compounds in the $R_3T_4X_4$ family. Transferred hyperfine field models suggest that the I_Pmmm' is the only group that is consistent with the ^{119}Sn Mössbauer results. We derive a samarium moment of $0.47 \pm 0.10\ \mu_B$ on the Sm 4e site at 3 K.

Acknowledgments

This work was supported by grants from the Natural Sciences and Engineering Research Council of Canada and Fonds pour la formation de chercheurs et l'aide à la recherche, Québec. PR wishes to thank the MIUR for the for research support: PRIN2004 'Caratterizzazione Chimico fisica di composti intermetallici in forma di bulk e in forma di film'. JMC is grateful to the Canada Research Chairs programme and the Canada Foundation for Innovation for their support.

References

[1] Voyer C J, Ryan D H, Napoletano M and Riani P 2007 *J. Phys.: Condens. Matter* **19** 156209
[2] Perry L K *et al* 2006 *J. Appl. Phys.* **99** 08J502
[3] Wawrzyńska E *et al* 2004 *J. Phys.: Condens. Matter* **16** 7535
[4] Perry L K *et al* 2006 *J. Phys.: Condens. Matter* **18** 5783
[5] Boulet P *et al* 1999 *Intermetallics* **7** 931
[6] Rieger W 1970 *Monatsch. Chem.* **101** 449
[7] Wawrzyńska E *et al* 2003 *J. Phys.: Condens. Matter* **15** 5279
[8] Szytuła A *et al* 2004 *J. Alloys Compounds* **367** 224
[9] Ryan D H, Cadogan J M, Gagnon R and Swainson I P 2004 *J. Phys.: Condens. Matter* **16** 3183
[10] Wawrzyńska E *et al* 2003 *Solid State Commun.* **126** 527
[11] Perry L K *et al* unpublished
[12] Mazzone D, Riani P, Napoletano M and Canepa F 2005 *J. Alloys Compounds* **387** 15
[13] Larson A C and von Dreele R B 2000 *Report LAUR* 86-748 Los Alamos National Laboratory
[14] Toby B H 2001 *J. Appl. Crystallogr.* **34** 210
[15] Voyer C J and Ryan D H 2006 *Hyperfine Interact.* **170** 91
[16] Potter M, Fritzsche H, Ryan D H and Cranswick L M D 2007 *J. Appl. Crystallogr.* **40** 489
[17] de Wijn H W, van Diepen A M and Buschow K H J 1973 *Phys. Rev.* B **7** 524
[18] Buschow K H J, van Diepen A M and de Wijn H W 1973 *Phys. Rev.* B **8** 5134
[19] Stewart A M 1972 *Phys. Rev.* B **6** 1985
[20] Le Cäer G, Malaman B, Venturini G and Kim I B 1982 *Phys. Rev.* B **26** 5085
[21] Perry L K, Ryan D H and Venturini G 2007 *Phys. Rev.* B **75** 144417